Journal of Applied Electrochemistry **31**: 685–692, 2001.
© 2001 *Kluwer Academic Publishers. Printed in the Netherlands.*

Influence of polyethoxylated additives on zinc electrodeposition from acidic solutions

G. TREJO, H. RUIZ, R. ORTEGA BORGES and Y. MEAS
Centro de Investigación y Desarrollo Tecnológico en Electroquímica (CIDETEQ), Parque Tecnológico Querétaro – Sanfandila, Apartado Postal 064, Pedro Escobedo, Querétaro Mexico CP 76700

Received 7 January 2000; accepted in revised form 30 January 2001

Key words: additives, electrocrystallization, electrodeposition, zinc alloys

Abstract

The influence of several ethoxylated additives (ethyleneglycol and polyethyleneglycol polymers of different molecular weights) on the nucleation, growth mechanism and morphology of zinc electrodeposited from an acidic chloride bath is reported. The electrochemical study was carried out using cyclic voltammetry, inversion potential and chronoamperometric techniques. The dimensionless graphs model was applied to analyse the nucleation process and the results showed that the studied additives have a blocking effect on the electrodeposition of zinc. This effect occurs in the first stages of the nucleation process and is dependent on the molecular weight of the additive. Changes induced by the presence of additives in the morphology and grain size of the deposits were observed using SEM analysis. Results show that the presence of additives modifies the nucleation process and determines the final properties of the deposits.

1. Introduction

The use of additives in electrodeposition solutions is extremely important due to their influence on the growth and structure of the resulting deposits. The presence of additives has been shown to influence physical and mechanical properties of electrodeposits such as grain size, brightness, internal stress, pitting and even chemical composition [1].

The role of additives in the electrodeposition process is not clearly understood and its investigation has been mostly empirical. In recent years, the formal study of the effect of additives has increased, especially for the electrodeposition of the most commonly used metals in metal finishing such as zinc, copper and nickel. Additives are frequently assumed to act as catalysts or inhibitors in the electrodeposition process by increasing the tendency of metal ions to form complexes and/or raising the activation polarization of single ions by blocking the active sites on the substrate [2].

Additives are often organic polymeric compounds of high molecular weight or compounds able to form colloidal suspensions which are more effective than small ions or single molecules [3]. Polyethoxylated compounds are common additives for electrodeposition of bright zinc from acidic solutions [4]. However, their influence on the nucleation and growth mechanism of the first crystals and on the morphological characteristics of the deposits is still not clear, and has been little studied. Stoychev and Rashkov [5], for instance, established that the addition of polyethoxylated additives to sulfuric acid electrolytes increases the overpotential of copper electrodeposition. Aragón et al. [6] reported similar results for the electrodeposition of tin. On the other hand, studies on the differential capacity of polycrystalline electrodes in the presence of additives have shown that ethoxylated compounds are partially adsorbed [7]. Studies by scanning tunneling microscopy (STM) of the underpotential deposition of copper on platinum [8] have shown that the presence of additives induces a change from an isolated growth mechanism to a mechanism involving the formation of stacks of layers.

The aim of this work is to study the influence of polyethoxylated additives on the electrodeposition of zinc on glassy carbon (GC) substrates from acidic baths concentrated in chlorides. The studied additives were ethyleneglycol polymers (polyethyleneglycol, PEG) of different molecular weights: 400, 8000 and 20 000 g mol^{-1} and ethyleneglycol which was used as a reference since it is the single unit present in all the evaluated polymeric compounds. GC was selected as the substrate on account of its high overpotential for hydrogen evolution. Electrochemical studies were carried out by cyclic voltammetry and by chronoamperometric techniques. A scanning electronic microscope (SEM) coupled to an energy dispersion spectrometric (EDS) probe was employed to study the morphology and composition of the deposits.

2. Experimental details

Zinc was electrochemically deposited from solutions containing 0.6 M $ZnCl_2$ (Merck), 2.8 M KCl (Merck) and 0.32 M H_3BO_3 (Merck). Potassium chloride was used to give a highly conductive electrolyte and boric acid was used as a buffer to prevent a rise in the interfacial pH. Several authors have reported that boric acid is also adsorbed at the substrate surface, suppressing hydrogen evolution and catalysing metal deposition [9–12]. The polyethoxylated additives were employed independently at a fixed concentration of 5×10^{-3} M. The composition of the solutions is given in Table 1. All reagents were analytical grade and the corresponding solutions were prepared with deionized water (18 MΩ cm). In all cases the pH of the working solutions was 5.0.

The electrochemical experiments were carried out using an EG&G Princeton Applied Research potentiostat/galvanostat (model 273A) coupled to a personal computer equipped with the EG&G M270 software for data acquisition.

The electrochemical studies were performed in a conventional three-electrode cell with a water jacket. The working electrode was a glassy carbon disc (0.07 cm^2 geometric area); a saturated calomel electrode (SCE) was employed as the reference electrode and a graphite rod was used as the counterelectrode. Prior to each experiment, the working electrode was polished to a mirror finish using alumina 0.05 μm (Buehler). After polishing, the electrodes were electrochemically pretreated in a solution containing 0.01 M $K_4Fe(CN)_6$ and 1 M KNO_3. This pretreatment gives a better electrochemical response and assures reproducibility. All experiments were performed under ultrapure nitrogen atmosphere (Linde). Temperature was controlled using a Cole Parmer water circulation system.

The morphology and chemical composition of the deposits were evaluated using a scanning electronic microscope (Jeol model DSM-5400 LV) coupled to an energy dispersion spectrometer (Kevex).

3. Results and discussion

3.1. *Thermodynamic study*

To characterize the chemical species present in the working solutions, a thermodynamic study of the zinc species that are stable in aqueous solution at the working conditions was carried out. A predominance diagram, pZn′ vs pH (pZn′ is the cologarithm of the total concentration of soluble zinc species) for the system Zn(II)/Cl/H_2O was obtained by using the graphical method reported by Rojas et al. [13–15] (Figure 1). This diagram was obtained from the reported thermodynamic formation constants [16] of complexes between Zn^{2+}, Cl^- and OH^- and applying the model of generalized equilibria [13–15] at the working conditions: 0.6 M total zinc concentration (pZn′ = 0.22, corresponding to all forms of the soluble zinc species: Zn^{2+}, $ZnCl^+$, $ZnCl_2$, $ZnCl_3^-$ and $ZnCl_4^{2-}$) and 2.82 M total chloride concentration (pCl′ = −0.45). No data are reported for the formation constants of complexes between zinc and the studied additives.

Table 1. Composition of the experimental solutions

Solution	Compositions
1	0.6 M $ZnCl_2$ + 2.8 M KCl + 0.38 M H_3BO_3 (basic solution)
2	No. 1 + 5×10^{-3} M ethyleneglycol (EG)
3	No. 1 + 5×10^{-3} M polyethyleneglycol 400 (PEG 400)
4	No. 1 + 5×10^{-3} M polyethyleneglycol 8000 (PEG 8000)
5	No. 1 + 5×10^{-3} M polyethyleneglycol 20 000 (PEG 20 000)

In Figure 1 the solid line represents the solubility equilibrium, corresponding to the boundary region between the insoluble zinc species (below this line) and the soluble zinc species (above this line). The dashed lines define the boundary between the predominance zones for the different soluble species. The soluble tetrachloride zinc complex, $ZnCl_4^{2-}$, is the predominant zinc species at the working conditions (pZn′ = 0.22 and pCl′ = −0.45) in the pH range 0 to 7. At higher pH, the predominant species is insoluble $Zn(OH)_2$.

In this way, it is possible to assume that at the working conditions the zinc reduction process involves the $ZnCl_4^{2-}$ species, according to the following reaction,

$$ZnCl_4^{2-} + 2e^- \rightarrow Zn(0) + 4\,Cl^- \qquad (1)$$

with an apparent normal potential $E^{\circ\prime}_{ZnCl_4^{2-}/Zn(0)}$ (vs SCE) that can be expressed as a function of pCl′ and pZn′ by the following equation, in a similar manner to the case where additives are absent [17]:

$$E^{\circ\prime}_{ZnCl_4^{2-}/Zn(0)} = -1.01 + 0.12pCl' - 0.03pZn' \qquad (2)$$

Application of Equation 2 is limited to the pH range 0–7 where $ZnCl_4^{2-}$ is the predominant species. For the

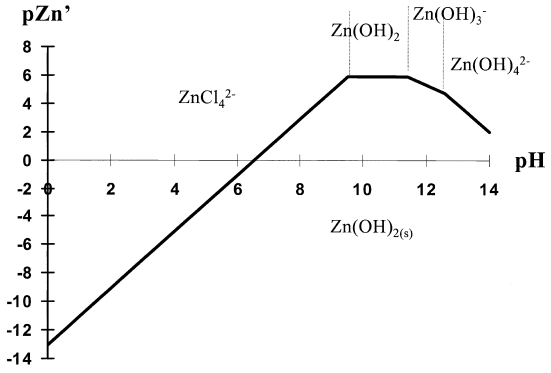

Fig. 1. Predominance diagram (pZn′ vs pH) for the system Zn(II)′/Cl/H_2O constructed for $pCl^- = -0.45$.

working conditions (pCl′ = −0.45, pZn′ = 0.22 and pH = 5.0), $E^{o\prime}_{ZnCl_4^{2-}/Zn(0)}$ has a value of −1.070 V vs SCE.

3.2. *Voltammetric study*

The voltammetric study was carried out in the potential range 0.8 to −1.6 V vs SCE. Figure 2 shows the voltammograms obtained in the absence and presence of each additive. During the cathodic scan only a reduction peak (Ic) was observed. This peak is associated with the reduction of Zn(II) to Zn(0). Likewise, in the anodic scan, an oxidation peak (Ia) is observed, related to the oxidation of Zn(0) formed during the cathodic scan.

It is important to note that the cathodic response is typical of a metallic electrodeposition process involving nucleation. In these cases, an overpotential is required to form the first nuclei on the substrate surface, and afterwards the current density quickly increases. When the potential scan is reversed, a higher cathodic current is observed, due to the growth of the first nuclei, producing a crossover point between the cathodic and anodic scans. This crossover point, the crossover potential (E_{co}), is also observed in the presence of additives, but the potential of the cathodic peak (E_{cp}) is shifted to more cathodic values as the molecular weight of the additive increases.

Results of the study of the variation of the current density of the cathodic peak (j_{cp}) as a function of the scan potential rate (v) are shown in Figure 3. The linear relation observed between j_{cp} and $v^{1/2}$ indicates that the reduction process is controlled by mass transfer [18]. On the other hand, the value negative of the cathodic current density (j_{cp}) at $v^{1/2} = 0$, is consistent with a deposition process involving a nucleation mechanism controlled by mass transfer [19]. Similar behaviour is observed for all the studied additives, but with lower values of the absolute value of j_{cp}. It is important to note that the observed decrease is dependent on the molecular weight of the additive. This fact is attributed to the adsorption of the additives at the electrode surface, which produces a decrease in the electrode active area.

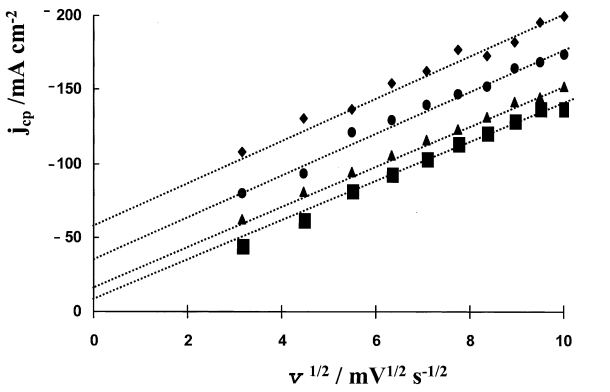

Fig. 3. Variation of the peak current density (j_{cp}) with the sweep potential rate for zinc deposition on glassy carbon from a 0.6 M $ZnCl_2$ + 2.8 M KCl + 0.32 M H_3BO_3 solution (pH 5.0), with and without additives added to the deposition solution: (◆) solution 1, (●) solution 2, (▲) solution 4 and (■) solution 5.

To determine the type of kinetic control involved in the deposition of zinc, a voltammetric study was carried out at different negative switching potentials (E_λ), where E_λ was selected so that $E_\lambda > E_{cp}$. Under these conditions, the number of the nuclei formed can be modulated and the deposition process is not diffusion controlled.

During the cathodic scan, a slight increase in current density was observed before the reduction peak. This current is associated with hydrogen evolution.

Figure 4 shows a family of voltammetric curves obtained at different values of E_λ. E_{co} is independent of E_λ, indicating that under the studied conditions the electrodeposition process is controlled by charge transfer according to Fletcher's theory [20, 21]. In these cases, E_{co} can be assumed to be the equilibrium potential of the metallic ion/metal system ($E^{0\prime}_{M^{n+}/M}$) and, from the results of the thermodynamic study (Section 3.1), the $ZnCl_4^{2-}/Zn(0)$ system can be postulated to be the system involved in the electrodeposition process.

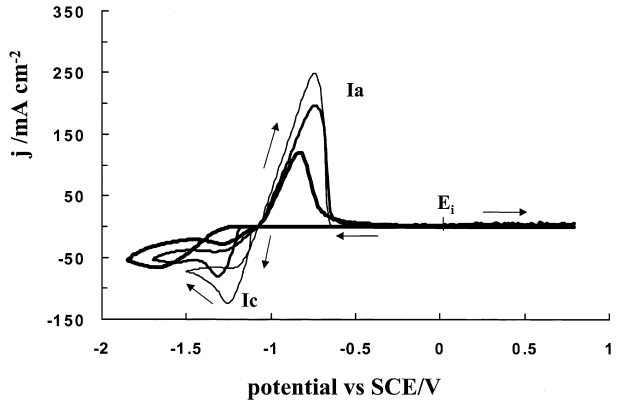

Fig. 2. Typical voltammograms for zinc deposition on glassy carbon from a 0.6 M $ZnCl_2$ + 2.8 M KCl + 0.32 M H_3BO_3 solution. $v = 40$ mV s^{-1}, pH 5.0 in the presence of different polyethoxylated additives: (—) solution 1, (▬) solution 4 and (▬) solution 5.

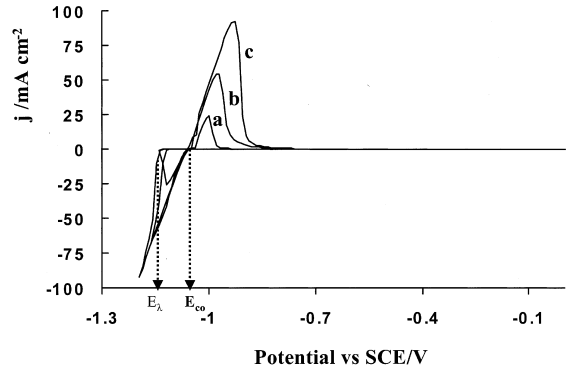

Fig. 4. Typical voltammograms of zinc deposition on glassy carbon from solution 2, showing the switching (E_λ) and the crossover potentials (E_{co}): (a) $E_\lambda = -1.13$, (b) $E_\lambda = -1.15$, (c) $E_\lambda = -1.18$ V vs SCE, $v = 40$ mV s^{-1}.

Table 2 shows the average values of E_{co} obtained for the studied solutions, in the absence and presence of additives. The E_{co} values observed are close to each other and could be assumed to be equal to the thermodynamic potential ($E^{o\prime}_{ZnCl_4^{2-}/Zn(0)} = -1.07$ V vs SCE) previously calculated under these conditions. It is possible to conclude that the reduction reaction involves the majority zinc chloride species $ZnCl_4^{2-}$, as expected at high chloride concentration (2.8 M) when compared to the concentration of additives (5×10^{-3} M). Thus, under these conditions, the reduction of Zn(II) in the presence and absence of additives may be represented by Equation 1.

Table 2 also shows the overpotential values ($\eta, \eta = E_{cp} - E_{co}$) observed in the presence and absence of additives. When additives are present, a higher overpotential is observed and the absolute value of the overpotential increases as the molecular weight of the additive is increased. This suggests that the additive acts at the interface, creating a barrier in the proximity of the electrode surface that has a blocking effect on electrodeposition. Therefore, additional energy is required to discharge the metal ions. Thus, the presence of polyethoxylated additives increases the deposition overpotential and decreases the current density of the cathodic peak.

3.3. *Chronoamperometric study*

The chronoamperometric study was performed in the potential range −1.2 to −1.8 V vs SCE. A family of potentiostatic transients obtained in the presence of PEG 400 is shown in Figure 5(a). The transients are typical of a nucleation process [22–25] and similar behavior was observed for all solutions. At the short times, a rise in current density is observed until a maximum value (j_m) is reached. This behaviour can be explained in terms of the growth and stabilization of the first nuclei. After reaching a maximum value, the current density decays, behaviour typical of a diffusion controlled process. Similar results are observed for the other solutions, as shown in Figure 5(b). The transients were obtained at the same potential (−1.3 V vs SCE) except for solution 5, for which a more cathodic potential (−1.55 V vs SCE) was required to reach j_m. In the corresponding Figure, j_m is observed at longer times in the presence of additives and decreases when the molecular weight of the additive is increased. These results are associated with the adsorption of the additive on the substrate surface, diminishing the active area and increasing the induction time required to form nuclei.

Table 2. Cathodic peak potential (E_{cp}), crossover potential (E_{co}) and overpotential (η) values associated with zinc deposition on glassy carbon from a 0.6 M $ZnCl_2$ + 2.8 M KCl + 0.32 M H_3BO_3 solution in the absence and in the presence of 5×10^{-3} M of additives, $v = 40$ mV s^{-1}, pH 5.0

Additive	E_{cp} vs SCE/V	E_{co} vs SCE/V	η/V
Without additive	−1.245	−1.068	−0.177
Ethyleneglycol (EG)	−1.289	−1.068	−0.221
PEG 400	−1.305	−1.072	−0.233
PEG 8000	−1.332	−1.070	−0.262
PEG 20 000	−1.690	−1.070	−0.620

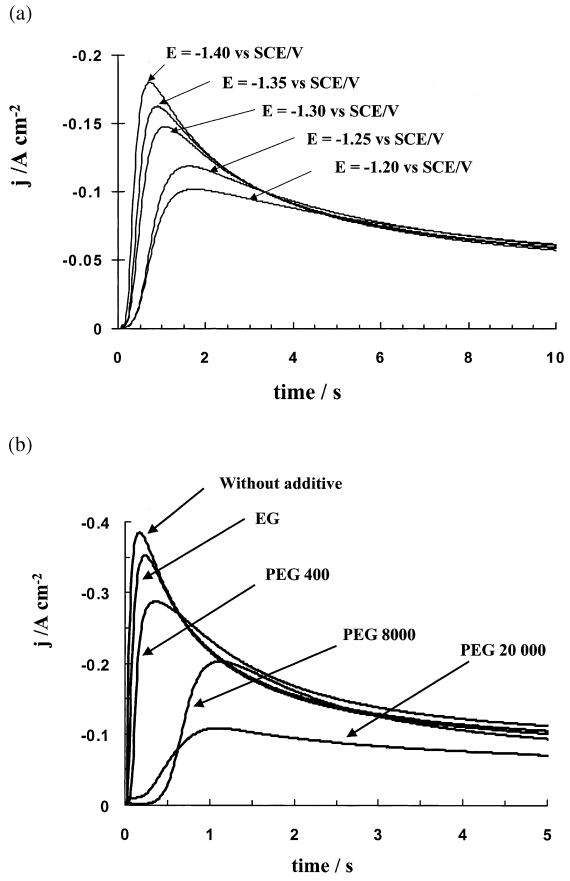

Fig. 5. (a) Typical family of potentiostatic transients obtained at different fixed potentials for zinc electrodeposition on glassy carbon from solution 2. (b) A family of potentiostatic transients of zinc electrodeposition on the glassy carbon electrode from the studied solutions. Solutions 1, 2, 3, 4, $E = -1.3$ V vs SCE, solution 5 (PEG 20 000), $E = -1.5$ V vs SCE.

To identify the nucleation mechanism, dimensionless curves were obtained from the potentiostatic transients and were compared with those obtained using the model of Scharifker et al. [22] for 3D instantaneous and progressive nucleation processes controlled by diffusion. For an instantaneous nucleation process, the model assumes a very high nucleation rate and the instantaneous coverage of all the active sites by nuclei. In this case, the process is described by the following equation (Equation 3):

$$\left(\frac{j}{j_m}\right)^2 = 1.9542\left(\frac{t}{t_m}\right)^{-1}\left\{1 - \exp\left[-1.2564\left(\frac{t}{t_m}\right)\right]\right\}^2 \quad (3)$$

For a progressive nucleation process, the number of nuclei is assumed to be a time dependent function and the corresponding equation (Equation 4) is:

$$\left(\frac{j}{j_m}\right)^2 = 1.2254\left(\frac{t}{t_m}\right)^{-1}\left\{1-\exp\left[-2.3367\left(\frac{t}{t_m}\right)^2\right]\right\}^2 \quad (4)$$

In both cases, j_m is the maximum current density and t_m is the time associated with j_m.

A comparison between the experimental and theoretical curves was carried out by plotting $(j/j_m)^2$ against t/t_m, the dimensionless parameters related to current and time. When an induction time (t_0) was observed, the experimental curves were corrected using the parameter $t' = t - t_0$ [26, 27]. This correction leads to better agreement between the experimental results and nucleation models.

Figure 6 shows the resulting dimensionless graphs. In the absence of additive (Figure 6(a)) the experimental results are well described by the instantaneous nucleation model. Similar results are obtained in the presence of EG and PEG 400.

In the presence of PEG 8000 (Figure 6(b)), however, a transition in the nucleation mechanism is clearly observed. Before the maximum in $(j/j_m)^2$, the experimental results are described by the progressive nucleation model and after this maximum by the instantaneous nucleation model. A similar mixed behavior is also observed with the PEG 20 000 additive, but with a longer induction time. These results suggest that the induction time increases when the molecular weight of the additive is increased, indicating a higher blocking effect of the additive. A transition between the two nucleation mechanisms has been reported for nucleation and growth processes controlled by mass transfer [23, 24, 28].

The dimensionless graph model also allows estimation of the number density of formed nuclei, N_s, according to the following equations [22] (Equations 5–8).
For progressive nucleation:

$$N_s = \left(\frac{AN_o}{2k'D}\right)^{1/2} \quad (5)$$

$$k' = \frac{4}{3}\left(\frac{8\pi CM}{\rho}\right)^{1/2} \quad (6)$$

And for instantaneous nucleation:

$$N_s = \frac{1.2564}{t_m \pi k D} \quad (7)$$

$$k = \left(\frac{8\pi CM}{\rho}\right)^{1/2} \quad (8)$$

where A is the nucleation rate constant, N_o is the number density of sites, C is the metal ion concentration in the bath (in mol cm^{-3}), M and ρ are the atomic weight (in g mol^{-1}) and the density (in g cm^{-3}) of the deposited metal, respectively. The other symbols are in the notation currently used in electrocrystallization and are described elsewhere [22, 25].

To accurately estimate N_s from Equations 5 and 7, the diffusion coefficient (D_0) of Zn(II) was evaluated using the chronoamperometric technique in steady state diffusion conditions to account for the changes in kinematic viscosity (v) of the deposition solution caused by the presence of additives. The values of D_0 are shown in Table 3.

The variation of N_s as a function of applied potential is shown in Figure 7. N_s varies exponentially with applied potential and decreases in the presence of

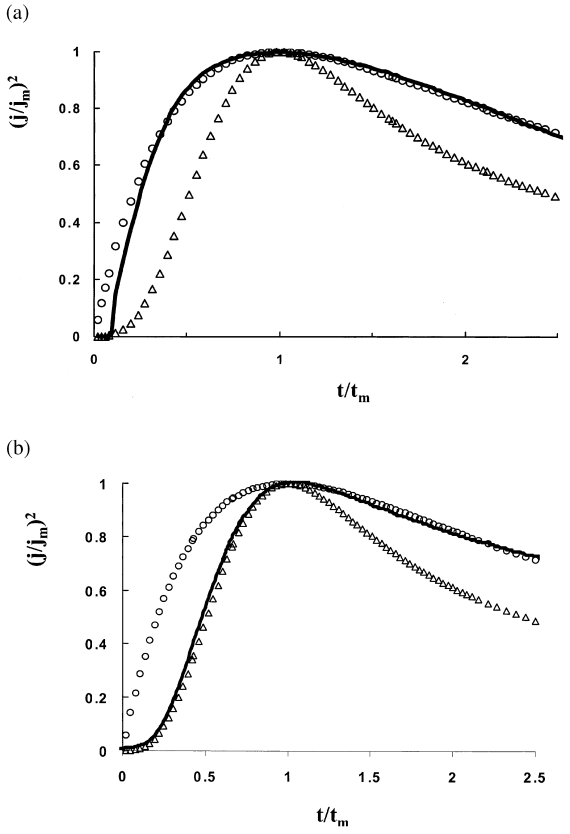

Fig. 6. Comparison between the theoretical dimensionless graphs for instantaneous (○○○) and progressive (△△△) nucleation to the experimental nucleation process (▬) for zinc deposition from a 0.6 M $ZnCl_2$ + 2.8 M KCl + 0.32 M H_3BO_3 solution in the absence (6a: solution 1) and in the presence of additives (6b: solution 4).

Table 3. Diffusion coefficient (D_0) and kinematic viscosity (v), values evaluated for a 0.6 M $ZnCl_2$ + 2.8 M KCl + 0.32 M H_3BO_3 solution at a fixed additive concentration of 5×10^{-3} M, pH 5.0

Additive	v/cm^2 s^{-1}	10^6 D_0/cm^2 s^{-1}
Without additive	0.00988	7.27
Ethyleneglycol (EG)	0.01005	5.43
PEG 400	0.01018	4.83
PEG 8000	0.01070	4.76
PEG 20 000	0.01264	4.59

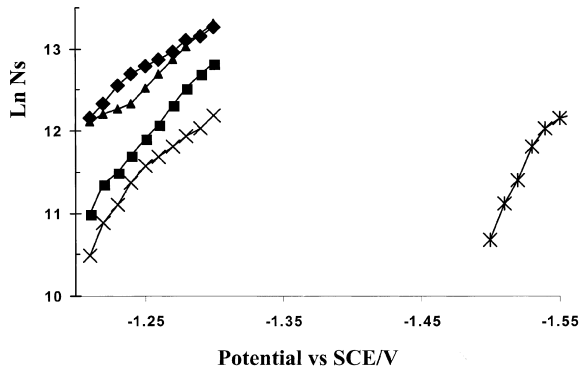

Fig. 7. Variation of the number density of formed nuclei (N_s) with the deposition potential from the studied solutions: (◆) solution 1, (▲) solution 2, (■) solution 3, (×) solution 4 and (*) solution 5.

additives, indicating an increase in the critical radius of the nuclei [29]. The decrease in N_s is greater when the molecular weight of the additive increases. This suggests that the polyethoxylated additives induce a decrease in the number density of the nuclei formed and an increase in the radius of these nuclei.

3.4. *Morphology of the deposits*

Zinc electrodeposits were analysed by SEM to determine the influence of the additives on the morphology in the initial deposition stages. The deposits were potentiostatically grown at −1.3 V vs SCE on GC for 40 s, from each solution, except for solution 5 where the deposition potential was −1.5 V vs SCE. Under these conditions, deposition is a diffusion controlled process (Section 3.3).

The morphology and grain size are both dependent on the presence of additives. In the absence of additives, the deposit is in the form of hexagonal plates (Figure 8(a)), as is typical for pure zinc electrodeposits [30, 31]. The size of these plates indicates an instantaneous nucleation mechanism. In the presence of EG, similar results are obtained but the plates show some degree of perpendicular orientation to the substrate surface (Figure 8(b)). In the presence of PEG 400, 8000 and 20 000 (Figure 8(c), (d) and (e), respectively), the deposits are formed by flakes grouped in clusters whose size is dependent on the molecular weight. The size increases from 14 to 22 μm^2 when the molecular weight of PEG is increased from 400 to 8000, but is drastically diminished when PEG 20 000 is used (6 μm^2), probably because the deposition potential (−1.5 V vs SCE) was not sufficiently cathodic for the stabilization of larger clusters. The increase in cluster size is expected on account of the blocking effect of the additives that causes a reduction in both the number of active sites and the nucleation rate. Similar effects, associated with a decrease in the nucleation rate, have been reported by Michailova et al. [32, 33] for copper electrodeposition in the presence of organic polyethoxylated additives.

Chemical analysis by EDS showed that the deposits were zinc. Chlorides were also detected and their presence may be associated with occluded solution in the deposit.

3.5. *Corrosion resistance*

To evaluate the influence of additives on the corrosion resistance, zinc electrodeposits were obtained on stainless steel AISI 1018 substrates of 1 cm^2 geometric area at −1.3 V vs SCE (solutions 1–4) and −1.5 V vs SCE (solution 5). During deposition, the amount of charge was measured using a charge integrator (Tacussel IG6-N). The deposition time was adjusted to obtain a final theoretical thickness of 12 μm. SEM analysis showed that the deposits have a morphology and grain size similar to those observed on GC under the same conditions (Section 3.4). The corrosion resistance of the deposits was evaluated by polarization measurements, according to the ASTM standard method [34] in a 3.5% w/v NaCl solution, previously saturated in oxygen by bubbling ultrapure oxygen for 1 h. The potential scan starts from a more cathodic potential ($E_{initial}$) than the corrosion potential ($E_{initial} = E_{corr} - 300$ mv) in the anodic direction until an anodic current of 5 mA was obtained.

The corrosion parameters are shown in Table 4. The deposits obtained in the presence of additives have a lower corrosion rate that those obtained in their absence. The lowest corrosion rate is observed with PEG 8000. The differences in corrosion behaviour are associated with the influence of the additive on properties of the deposits such as structure, grain size, compactness and adhesion.

4. Conclusions

The reduction mechanism of zinc from acidic concentrated chloride solutions involves the reduction of $ZnCl_4^{2-}$ to Zn(0). This reaction is not affected by the presence of polyethoxylated additives (EG and PEG 400, 8000 and 20 000) because the nature of the majority species of zinc in solution is not changed.

The adsorption and preferential orientation of additives at the electrode surface induce changes in the electrochemical parameters of the deposition process. An increase in the deposition overpotential and a decrease in the current density of the cathodic peak, for instance, are two clearly observed effects. Likewise, the electrode surface is partially blocked by the additives, causing a decrease both in the number of available active sites and the nucleation rate, resulting in an increase in grain size.

Additives also have a large influence on deposit morphology which changes from a plate structure to a nodular structure when additives are present. The corrosion resistance of deposits is also affected by additives. PEG 8000 gives the most compact deposits with a low corrosion rate.

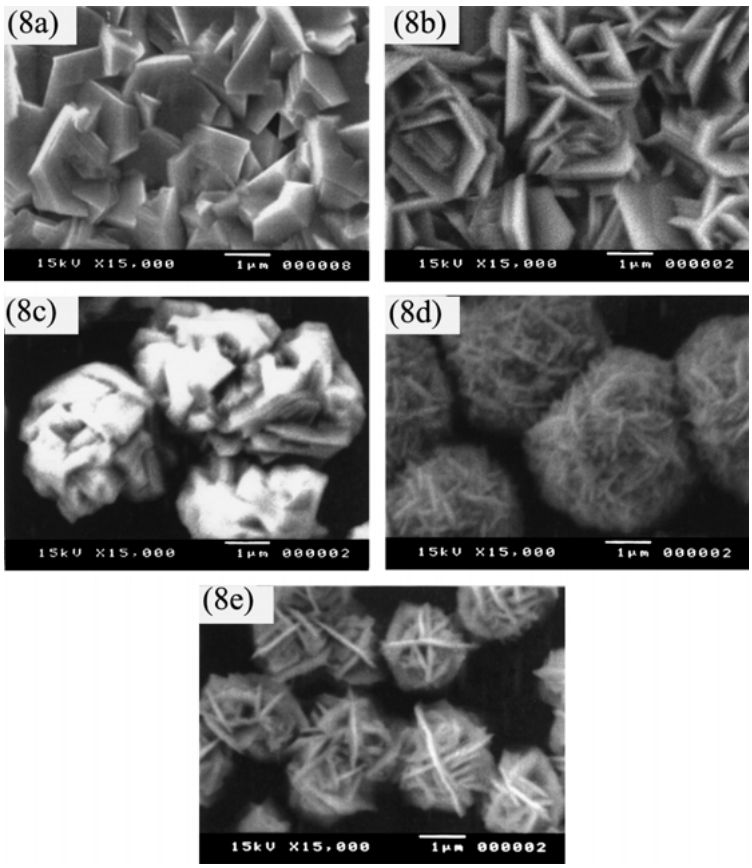

Fig. 8. SEM micrographs of zinc electrodeposited at −1.3 V vs SCE on glassy carbon from the studied solutions: (a) solution 1, (b) solution 2, (c) solution 3, (d) solution 4 and (e) solution 5 ($E = -1.5$ V vs SCE). Deposition time 40 s.

Table 4. Corrosion parameters in 3.5 wt % NaCl solutions for zinc electrodeposited on AISI 1018 steel from the studied solutions

Additive	Thickness /μm	E_{corr} vs SCE /V	j_{corr} /μA cm^{-2}	C.R. /mm year^{-1}
Without additive	12.20	−0.960	2.39	0.036
Ethyleneglycol (EG)	11.90	−0.950	1.97	0.029
PEG 400	11.90	−0.975	1.88	0.028
PEG 8000	11.90	−0.975	0.28	0.004
PEG 20 000	11.85	−0.975	1.07	0.016

The observed effects are dependent on the molecular weight of the polyethoxylated additive. Therefore, a judicious choice of additive will allow bright and homogeneous deposits to be obtained, with better characteristics than those obtained in the absence of additives.

Acknowledgements

This work was supported by the Consejo Nacional de Ciencia y Tecnología (CONACYT, México) (Programas SIHGO MT-20/95 y PCP 45). The authors are grateful to F. Manriquez for assisting in the SEM and EDS measurements and to L. Godínez Mora Tovar for his valuable suggestions and critical reading of the manuscript.

References

1. W.H. Safranek (Ed.), 'The Properties of Electrodeposited Metals and Alloys' (AESF, Florida, 1986).
2. J.W. Dini, 'Electrodeposition. The Material Science of Coatings and Substrates' (Noyes Publications, New Jersey, 1995).
3. D.A. Vermilyea, *J. Electrochem. Soc.* **106** (1995) 66.
4. Majid R. Kalantary, *Plat. Surf. Finish.* **80** (June 1994) 80.
5. D. Stoychev and S. Rashkov, *Commun. Dep. Chem. Bulg. Acad. Sci.* **9**(4) (1976) 618.
6. A. Aragón, M.G. Figueroa and R.E. Gana, *J. Appl. Electrochem.* **22** (1992) 558.
7. D. Stoychev, I. Vitanova, T. Vitanov and S. Rashkov, *Surf. Technol.* **7** (1978) 427.
8. M. Wünsche, R.J. Nichols, R. Schumacher. W. Beckman and H. Meyer, *Electrochim. Acta* **38** (1993) 647.
9. M. Pushpavanam and K. Balakrishnam, *J. Appl. Electrochem.* **26** (1996) 283.

10. C. Karwas and T. Hepel, *J. Electrochem. Soc.* **136** (1989) 1672.
11. R. Fratesi, G. Roventi, G. Giuliani and C.R. Tomachuk, *J. Appl. Electrochem.* **27** (1997) 1088.
12. H. Ruiz, G. Trejo, R. Ortega Borges and Y. Meas V., Memorias XIII Congreso de la Sociedad Iberoamericana de Electroquímica (1998) 580.
13. A. Rojas and I. González, *Anal. Chim. Acta* **187** (1986) 279.
14. A. Rojas-Hernández, M.T. Ramírez and I. González, *Anal. Chim. Acta* **278** (1993) 321.
15. A. Rojas-Hernández, M.T. Ramírez and I. González, *Anal. Chim. Acta* **278** (1993) 335.
16. M. Smith and A.E. Martell, 'Critical Stability Constants', Vol. 4 (Plenum Press, New York, 1979).
17. G. Trejo, R. Ortega Borges, Y. Meas V., E. Chainet, B. Nguyen and P. Ozil, *J. Electrochem. Soc.* **14** (1998) 4090.
18. A.J. Bard and L.R. Faulkner, 'Electrochemical Methods: Fundamental and Applications' (J. Wiley & Sons, New York, 1980).
19. G.J. Hills, D.J. Hills, D.J. Schiffrin and J. Thompson, *Electrochim. Acta* **19** (1974) 657.
20. S. Fletcher, *Electrochim. Acta* **28** (1983) 917.
21. S. Fletcher, C.S. Halliday, D. Gates, M. Westcott, T. Lwin and G. Nelson, *J. Electroanal. Chem.* **159** (1983) 267.
22. B.R. Scharifker and G. Hills, *Electrochim. Acta* **28** (1983) 879.
23. G. Gunawardena, G. Hills and I. Montenegro, *J. Electroanal. Chem.* **184** (1985) 371.
24. G. Gunawardena, G. Hills, I. Montenegro and B. Scharifcker, *J. Electroanal. Chem.* **138** (1982) 225.
25. B.R. Scharifker and J. Mostany, *J. Electroanal. Chem.* **177** (1984) 13.
26. P.M. Rigano, C. Mayer and T. Chierchie, *J. Electroanal. Chem.* **248** (1988) 219.
27. M. Palomar-Pardave, I. González, A.B. Soto and E.M. Arce, *J. Electroanal. Chem.* **443** (1998) 125.
28. M. Sánchez Cruz, F. Alonso and J.M. Palacios, *J. Appl. Electrochem.* **23** (1993) 364.
29. G. Trejo, A.F. Gil and I. González, *J. Electrochem. Soc.* **142** (1995) 3404.
30. G. Barceló, M. Sarret, C. Müller and J. Pregonas, *Electrochim. Acta* **43** (1998) 13.
31. H. Yan, J. Downes, P.J. Boden and S.J. Harris, *J. Electrochem. Soc.* **143** (1996) 1577.
32. E. Michailova, I. Vitanova, D. Stoychev and A. Mielchev, *Electrochim. Acta* **38** (1993) 2455.
33. E. Michailova, I. Vitanova, D. Stoychev and A. Mielchev, *J. Electroanal. Chem.* **366** (1994) 195.
34. P.C. Fazio, E.L. Gutman, S.L. Kauffman, J.G. Kramer, C.M. Leinweber, V.A. Mayer, P.A. McGee (Eds), ASTM G5. Standard reference test for making potentiostatic and potentiodynamic anodic polarization measurementes, *in* 'Annual Book of ASTM Standards, Vol. 03.02 Wear and Erosion, Metal Corrosion' (ASTM, Philadelphia, 1993), p. 71.